

Metallic glass thin films for potential biomedical applications

Neelam Kaushik,¹ Parmanand Sharma,² Samad Ahadian,¹ Ali Khademhosseini,^{1,3,4,5,6} Masaharu Takahashi,⁷ Akihiro Makino,² Shuji Tanaka,⁸ Masayoshi Esashi¹

¹WPI-Advanced Institute for Materials Research (WPI-AIMR), Tohoku University, Sendai 980–8577, Japan

²Research and Development Center for Ultra High Efficiency Nano-crystalline Soft Magnetic Materials, Institute for Materials Research, Tohoku University, Sendai 980–8577, Japan

³Department of Medicine, Center for Biomedical Engineering, Brigham and Women's Hospital, Harvard Medical School, Cambridge, Massachusetts 02139

⁴Harvard–MIT Division of Health Sciences and Technology, Massachusetts Institute of Technology, Cambridge, Massachusetts 02139

⁵Wyss Institute for Biologically Inspired Engineering, Harvard University, Boston, Massachusetts 02115

⁶Department of Maxillofacial Biomedical Engineering and Institute of Oral Biology, School of Dentistry, Kyung Hee University, Seoul 130–701, Republic of Korea

⁷Research Center for Ubiquitous MEMS and Micro Engineering, AIST, Tsukuba 305–8564, Japan

⁸Graduate School of Engineering, Tohoku University, Sendai 980–8579, Japan

Received 3 July 2013; revised 28 January 2014; accepted 18 February 2014

Published online 8 March 2014 in Wiley Online Library (wileyonlinelibrary.com). DOI: 10.1002/jbm.b.33135

Abstract: We introduce metallic glass thin films (TiCuNi) as biocompatible materials for biomedical applications. TiCuNi metallic glass thin films were deposited on the Si substrate and their structural, surface, and mechanical properties were investigated. The fabricated films showed good biocompatibility upon exposure to muscle cells. Also, they exhibited an average roughness of <0.2 nm, high wear resistance, and high mechanical properties (hardness ~6.9 GPa and reduced modulus ~130 GPa). Top surface of the TiCuNi films was shown to be free from Ni and mainly composed of a thin titanium oxide layer, which resulted in the high surface biocom-

patibility. In particular, there was no cytotoxicity effect of metallic glass films on the C2C12 myoblasts and the cells were able to proliferate well on these substrates. Low cost, viscoelastic behavior, patternability, high electrical conductivity, and the capability to coat various materials (e.g., nonbiocompatible materials) make TiCuNi as an attractive material for biomedical applications. © 2014 Wiley Periodicals, Inc. *J Biomed Mater Res Part B: Appl Biomater*, 102B: 1544–1552, 2014.

Key Words: thin films for biomedical use, metallic glass thin films, tissue engineering

How to cite this article: Kaushik N, Sharma P, Ahadian S, Khademhosseini A, Takahashi M, Makino A, Tanaka S, Esashi M. 2014. Metallic glass thin films for potential biomedical applications. *J Biomed Mater Res Part B* 2014;102B:1544–1552.

INTRODUCTION

Materials required for biomedical applications are selected by different criteria, such as mechanical properties, biocompatibility, and their ability to be shaped into desired shapes. Available traditional materials for biomedical applications are limited. As a result, a significant interest has been drawn to develop novel, functional, and biocompatible materials,^{1–4} which can promise asymptomatic and long-term use in the body. A variety of medical devices, such as hip and knee joints, coronary stents, heart valves, and intraocular lenses, have been successfully implanted in the human body. The materials of the implants are supposed to interact with the body's tissues and organs and to have potential anti-corrosive property due to the body's environment. Coating the implants with protective films, can reduce the corrosion and wear problems, which may extend the life-

time of implants for the benefit of patients. Thin films can be deposited on the implantable devices in order to facilitate and improve the integration of these devices with the body. For example bioinert/biocompatible hermetic encapsulation coatings are needed to protect Si microchips from chemical interactions with body fluids to avoid device failure and undesirable biological effects. So by encapsulation or protective coatings, implantation of Si microchips in human body parts is feasible.

Among the materials, metallic glasses have been emerging as a new class of biomaterials.⁵ The most attractive properties of metallic glasses include high strength, elasticity, corrosion resistance, and unique processing capabilities.⁶ These unique properties of metallic glasses result from their amorphous structure. Because of this amorphous structure they are free from grains and grain boundaries. Therefore,

Correspondence to: N. Kaushik (e-mail: neelam@mems.mech.tohoku.ac.jp)

Contract grant sponsor: World Premier International Research Center Initiative (WPI), MEXT, Japan

high-resolution surface textures or patterns on metallic glasses can be attained. Moreover, precise fabrication of complex three-dimensional geometries can be achieved because of the thermoplastic properties of these materials at super cooled liquid temperatures where metallic glasses undergo drastic softening (super-plasticity).^{6–8} Metallic glass thin films can be a new material for biomedical micro devices formed by thermoforming. Recently there are several reports of application based on thermoformed microdevices using polymers.⁹ The polymer in some application can be replaced by metallic glass thin films for more robust applications. Moreover biomimetic micro- or nanoscale surface topographies can be obtained by imprinting of metallic glass films for the microdevices. In the past 20 years, a wide range of glassy alloys has been developed based on Zr-, Fe-, Cu-, Ni-, Mg-, Pd-, Au-, Pt-, and Ti-based^{10–24}; however, few studies have recently been reported regarding the biocompatibility of these metallic glasses.^{25–27} Metallic glassy alloys have shown better corrosion properties in the physiological conditions compared to commonly used metallic biomaterials. *In vitro* studies have also found that metallic glasses supported similar or better cell adhesion and proliferation of NIH 3T3 embryonic mouse fibroblasts compared to commercial biomedical alloys.^{5,25,26} Metallic glasses were also reported to elicit better bioactivity than their crystalline counterparts.⁵ Their enhanced bioactivity, high corrosion resistance, polymer-like formability, and excellent mechanical properties suggest them as promising biomaterials. However, major hurdles still remain such as challenges in their production and lack of plastic deformation. Note that biocompatible metallic glasses can be made up to thickness or diameter of nearly tens of millimeters.

In this work, we try to explore the biocompatibility of metallic glass thin films as protective coatings for implants and also study the fabrication and imprinting of these metallic glass thin films. Ti-based metallic glassy alloy system (Ti₅₀Cu₄₂Ni₈) is considered in this study as Ti is recognized as a biocompatible element. The Ti-based glassy alloys are reported to have relatively low cost, low density, high specific strength and reasonable Young's modulus, good corrosion resistance, and large super cooled liquid region.^{28–30} The latter characteristic allows a large temperature window for three-dimensional shaping of the material. Because of their high flexibility, they can provide suitable substrates to assess effects of different topographies on cellular behaviors, such as cell adhesion, growth, and differentiation.^{31,32} In addition, inherent electrical conductivity of the metallic glass thin films could make them an attractive substrate to engineer the tissues for electro-active cells, such as muscle^{33–36} and cardiac cells.^{37,38} For TiCuNi metallic glassy alloy problem might arise as it contains some amount of nickel in it. Nickel is known to have toxic effects both *in vitro* and *in vivo* but less than Co or Vanadium, which are frequently used in implant alloys.³⁹ Nickel is the major cause of allergic contact dermatitis.⁴⁰ However, the amount of its release highly depends on material surface treatment. For instance, Nitinol contains 50% of nickel in the alloy and many reports claimed that with some special

surface treatments, the biocompatibility of Nitinol is at least equivalent to Co-Cr and stainless steel alloys and comparable to the titanium.^{41–43} These later metals are routinely used in implants. Presence of Cu in the present alloy might be a problem, but Cu is an essential trace mineral that is vitally important for both physical and mental health. Chronic (long-term) effect of Cu exposure can damage the liver and kidneys as free Cu causes toxicity that generates reactive oxygen species that can damage proteins, and DNA. It was observed that with some surface treatment in the presence of Cu on the top surface of the material can be avoided that do not pose any threat for toxicity. The imprinting experiment in the present study drastically reduced the presence of Cu on the film surface.

Here, we report the deposition of TiCuNi glassy thin films on the Si substrates and measure their properties, such as mechanical, surface chemistry, biocompatibility, and the ability for micro-formability.

MATERIALS AND METHODS

Materials and their characterizations

A metallic alloy target (50 mm in diameter and 3 mm in thickness) with a composition of Ti₅₀Cu₄₂Ni₈ was made using an arc melting technique. The alloy target was melted several times to make the homogenous distribution of the elements in the target. TiCuNi metallic glass thin films (thickness ~1 μm) were deposited on the Si (100) substrate at the room temperature using a RF-magnetron sputtering. The substrate was water cooled during the deposition. The sputtering chamber was evacuated to a base pressure of ~10⁻⁵ Pa. The films were deposited at a sputtering pressure and power of ~0.4 Pa and 100 W, respectively. High purity (grade 1) argon was used as the sputtering gas. The phase identification and thermal characteristics of the films were examined by the X-ray diffractometer (Rigaku: RINT—Ultima III, Japan) and differential scanning calorimetry (DSC), respectively. For DSC measurements, films were deposited on the NaCl substrate. Free standing film was obtained by dissolving the NaCl substrate in water. The compositional analysis of the as-deposited film was done using the electron probe micro analyzer (EPMA). Surface chemistry of as-deposited and imprinted film samples were analyzed using the X-ray photoelectron spectroscopy (XPS). Nanomechanical testing system (UBI, Hysitron, USA) with a Berkovich diamond indenter was used to study the mechanical properties of the films.

Si mold fabrication and imprinting of TiCuNi films

Si molds with periodic patterns of 3.2–20 μm in width and ~10 μm in depth were prepared by the standard photolithography and dry etching. Imprinting tests were carried out using a desktop imprinting equipment with the maximum load of 1.8 kN and the maximum temperature of 700°C. The sample size was ~10 × 10 mm². The imprinting temperature was ~400°C, which was determined from the result of the DSC measurement. Force applied during imprinting was ~1.8 kN. The film was heated to the required imprinting temperature in vacuum (<10⁻³ Pa), and then the mold was

pressed against the film. Following the specified imprinting time, the film was cooled to the temperature of its $T_g - 30^\circ\text{C}$ in about 2 min, and removed from the mold.

The surface morphologies and microstructure of the imprinted Ti-based metallic glass thin films were examined using a field-emission scanning electron microscope (FE-SEM) and atomic force microscope (AFM), respectively.

Cell culture

C2C12 myoblasts as purchased from the American Type Culture Collection (ATCC) were cultured in the high-glucose contained DMEM (Invitrogen, USA) supplemented with 10% fetal bovine serum (Bioserum, Japan) and 1% penicillin/streptomycin (Sigma-Aldrich, USA). The C2C12 myoblasts were trypsinized using the 0.25% trypsin/0.1% EDTA (Invitrogen, USA) when they reached 70–80% confluency. The cells were kept at a standard cell culture incubator (Sanyo, Japan) at 37°C with a 5% CO_2 atmosphere.

Cell seeding and growth on the metallic glass thin films

Prior to the cell seeding, the metallic glass thin films were cleaned as to sonicate with ethanol for 10 min followed by drying with the nitrogen gas. They were then sterilized using the UV lamp of cell culture hood for 1 h. For cell culture on the films, the C2C12 myoblasts were trypsinized from the cell culture flask, counted, and resuspended in the culture medium at a density of 1×10^5 cells mL^{-1} . Then, 100 μL of this suspension was pipetted on 1 cm^2 of the films and incubated for 20 min at 37°C to allow for the cell adhesion to the films. Cells loaded on the metallic glass thin films were then cultured after adding sufficient culture medium. The culture medium was replenished every 24 h for the samples. Following the protocol described in our previous works,^{44,45} after 1 day of culture, the muscle cells were fixed by immersing in 4% paraformaldehyde for 30 min and then frozen by liquid nitrogen. They were then dehydrated for further SEM measurements using the SEM machine (JEOL JIB-4600F, Japan).

Immunostaining of C2C12 myoblasts on the metallic glass films

After 1 day of culture, the C2C12 skeletal muscle cells were fixed with 4% paraformaldehyde for 12 min, followed by washing with Dulbecco's phosphate-buffered saline (DPBS). The cells were treated with 0.3% Triton X-100 for 5 min at room temperature to open the cells membrane. After that, they were exposed to 5% bovine serum albumin dissolved in DPBS for 30 min. The samples were immunostained with 4,6-diamidino-2-phenylindole (DAPI) (Vector Laboratories, USA) and phalloidin (AlexaFluor® 594, Invitrogen, USA) as recommended by the manufacturers in order to reveal cell nuclei and filamentous F-actin, respectively. The stained cells pictures were taken using a fluorescence microscope (Carl Zeiss Observer Z.1, Germany).

Assessment of cell viability

Calcein AM/ethidium homodimer live/dead assay (Invitrogen, USA) was used to quantify the percentage of viable

cells according to the manufacturer's instructions. Calcein AM is a cell-permanent dye that is changed to the green fluorescent calcein in the live cells through the action of intracellular esterases. Ethidium homodimer is a DNA-binding dye that can enter the damaged membranes of dead cells and stain them as red. Calcein AM and ethidium homodimer fluorescence pictures were observed and recorded using the fluorescence microscope. At least five $10\times$ magnification images of two independent experiments were used to calculate the cell viability.

RESULTS AND DISCUSSION

Structural and thermal properties

A significant difference in the composition of thin films was observed for the films likely due to different sputtering rate of each element in the alloy. The average elemental composition of the as-deposited TiCuNi films measured by EPMA was found to be $\text{Ti}_{53}\text{Cu}_{36}\text{Ni}_{11}$, which is slightly different from the nominal target composition ($\text{Ti}_{50}\text{Cu}_{42}\text{Ni}_8$).⁴⁶

Figure 1(a) shows the X-ray diffraction patterns of a ~ 1 - μm thick TiCuNi/Si film deposited at the room temperature. The XRD pattern shows a broad diffraction peak at around $2\theta = 40^\circ$ confirming an amorphous structure. Surface roughness of the metallic glass thin film in the as-deposited state is also an important factor for fabricating nano- to micro patterns. Therefore, the surface of the Ti-based metallic glass film was analyzed by the atomic force microscopy. Inset of Figure 1(b) shows an AFM image of the thin films indicating smooth surface without grains and grain boundaries. The average surface roughness of the film was < 0.2 nm. Considering the average roughness for Si substrate (i.e., 1.61 nm), it is concluded that there was no degradation in the surface of the Ti-based metallic glass films as deposited on the Si substrate.

To demonstrate the capability of metallic glass thin films for the thermal imprinting, their thermal properties were evaluated. DSC curve of a TiCuNi thin film is shown in Figure 1(b). The glass transition temperature (T_g), the onset of crystallization temperature (T_x), and the super cooled liquid region (ΔT_x) of the films were 384, 430, and 46°C , respectively. The presence of a large super cooled liquid region required for the thermal imprinting confirms the possibility of fabrication of micro or nano structured surface patterns by this metallic glass thin film.

Patterning of TiCuNi thin films by the thermal imprinting technique

To confirm the imprintability or thermo-formability of the Ti-based glassy alloy thin films, the thermal imprinting was carried out using the Si molds. Figure 2(a–c) show the SEM images of the Si molds with feature sizes ranging from 3.2 to 20 μm . Two types of Si molds, one with square dot arrays and another with line and space (L&S) patterns were used. The glassy alloy thin film with a thickness of ~ 2 μm was pressed at temperatures ranging from T_g to $T_g + 26^\circ\text{C}$. The time for imprinting was fixed at 180 s. An anti-sticking layer was not coated on the mold surface because the

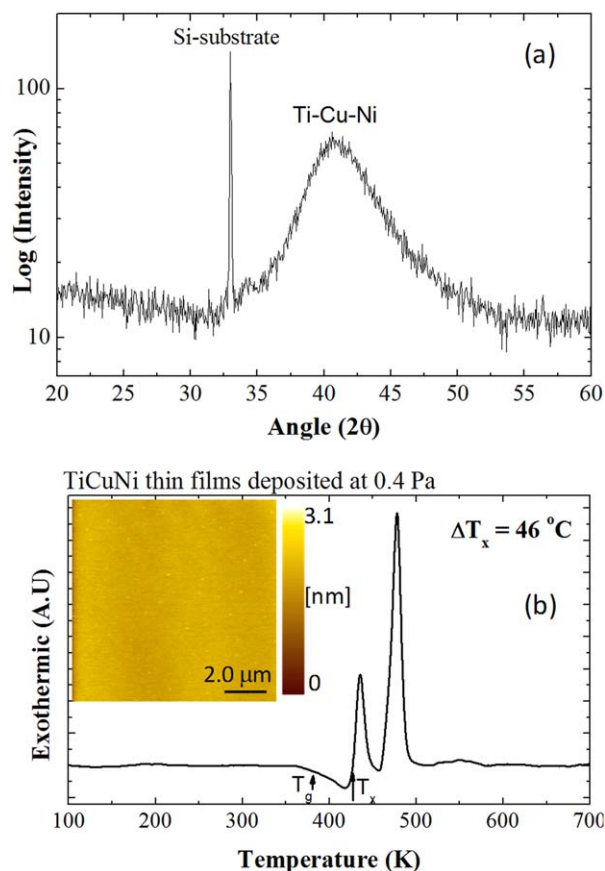


FIGURE 1. (a) X-ray diffraction pattern of a $\sim 1\text{-}\mu\text{m}$ thick TiCuNi /Si film deposited at room temperature, and (b) DSC curve showing well defined supercooled liquid region. Inset of (b) shows the topographic image of TiCuNi film. Grain free surface morphology in the image is typical for glassy thin films. [Color figure can be viewed in the online issue, which is available at wileyonlinelibrary.com.]

conventionally-used anti-sticking layers cannot withstand the imprinting temperatures of the glassy alloy.

Figure 3(a,b) are typical FE-SEM images of dot and L&S patterns on the Ti-based glassy alloy thin films imprinted at two different imprinting temperatures, that is, 400 and 410°C. The patterns on the master mold were precisely replicated on the films.

Further analysis of the imprinted patterns was carried out by the AFM. The left inset of Figure 3(c) shows the 3D topographic image of the L&S patterns. The complete filling of the grooves with TiCuNi during the imprinting was not achieved. Note that it may be feasible to simply increase the micro-pattern depth by increasing imprinting load and time. However, increasing the imprinting temperature above T_g may crystallize the glassy alloy films.

As shown in the left inset of Figure 3(c), the central parts of the imprinted lines exhibited a slight dip. A similar behavior has also been observed during the imprinting of polymeric materials.^{47,48} It seems that the contact angle between the thin film and the Si mold and the friction force at the interface with the mold are possible reasons for this result.⁴⁹ It was observed that the sidewalls of the mold significantly affected the top surface of the resulted patterns. The dual peak surface

morphology changes to a single peak when decreasing the pattern size. The contact angle might depend on the internal pressure and surface tension related to the wetting ability between the imprinted material and the mold. The friction force between the substrates might be also affected by the reaction between two surfaces. Note that sidewalls and the surface of the imprinted patterns are smooth and free from the granular structure [see the right inset of Figure 3(c)].

The XRD curves of the imprinted TiCuNi thin films also exhibited a broad hallow peak. The XRD and AFM results of the imprinted films and as-deposited films were almost similar, suggesting that the glassy structure of TiCuNi did not change after the imprinting process. However, a careful examination of the XRD patterns of the as-deposited and imprinted samples revealed a slight shift in the broad hallow peak. This may be due to the stress relaxation of the films after the heating process.⁵⁰

Surface analysis using X-ray photoelectron spectroscopy

Surface structure and chemical composition of the implanted materials have crucial roles in their function and

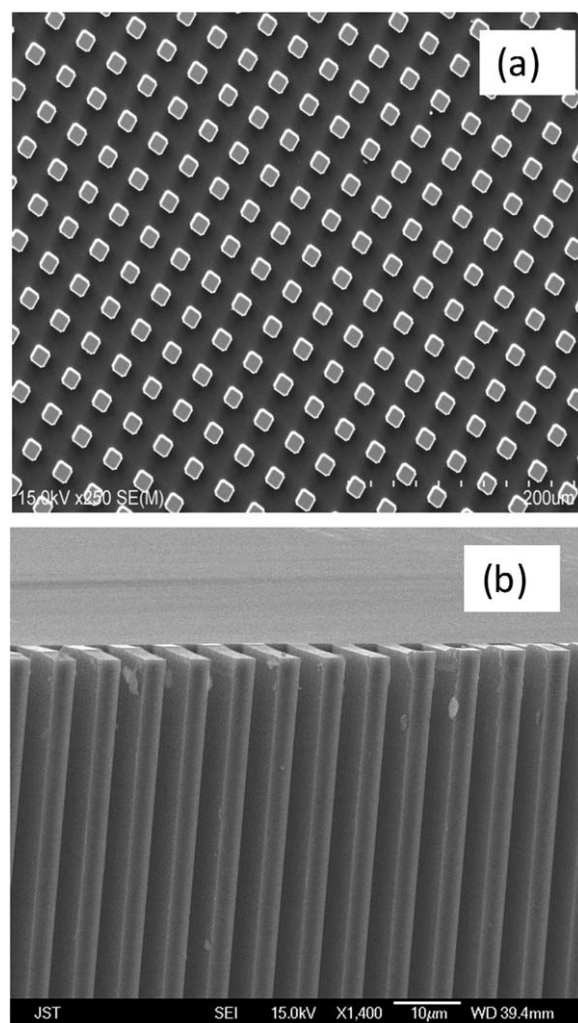


FIGURE 2. SEM images of two different types of Si mold; (a) square pillar, and (b) grating type.

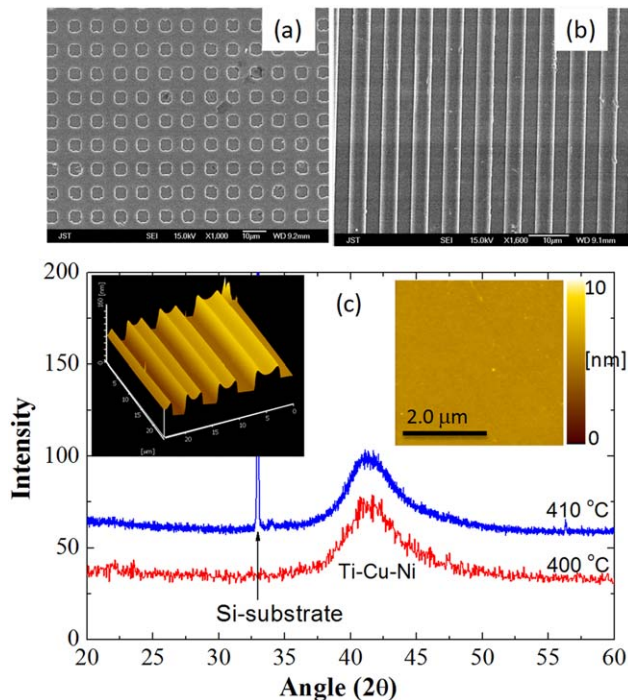


FIGURE 3. SEM images of imprinted TiCuNi metallic glass thin films (a) imprinted at 400°C, and (b) at 410°C. XRD patterns of imprinted films (c) suggest that the films are in glassy state. Inset of (c) shows the 3D topographic image (left side), and a small area 2D scan (right side) obtained from AFM. Very smooth and grain free surface of imprinted film is similar to as deposited film. [Color figure can be viewed in the online issue, which is available at wileyonlinelibrary.com.]

performance in biological conditions. Therefore, surface chemistry of fabricated metallic glass thin films was investigated. Furthermore, as-deposited and imprinted TiCuNi metallic glass thin films were studied using the X-ray photoelectron spectrometer (XPS). Measurements were performed by employing an Al K α (1486.6 eV) monochromated X-ray source. The survey spectra for as-deposited and imprinted TiCuNi metallic glass thin films on the Si substrate exhibited both Auger peaks (O KLL, Ti LMM, and Cu LMM), and XPS peaks (Ti, O, Ni, C, and Cu) (Figure 4). The peaks of Cu 3s and Cu 3p detected from the as-deposited TiCuNi film were weak and these peaks were disappeared in the case of imprinted TiCuNi film sample. The exact reasons for the absence of Cu and Ni peaks in imprinted TiCuNi thin film need further investigations. However, because of the strong affinity of Ti for oxygen and its higher concentration in the film compared to Cu and Ni, a rapid formation of titanium oxide to the film surface is expected. Enrichment of titanium oxide on the surface is also reported in the case of NiTi shape memory alloy.⁵¹ Narrow scan was performed for each element to get detailed information. Figure 4(a–c) demonstrate the spectra of Ti2p, Cu2p, and Ni2p for both as-deposited and imprinted TiCuNi metallic glass thin films. In Figure 4(a), Ti peak positions correspond to Ti⁴⁺ and Ti³⁺ oxidation states. One minor metallic peak (around 454 eV) was also observed in the case of as-deposited TiCuNi film; however, it was disappeared for the imprinted sample.

Similarly, metallic Ni peaks were observed [as shown in Figure 4(c)] for the as-deposited TiCuNi metallic glass thin films; however, the imprinted sample did not contain any metallic Ni. Figure 4(b) indicates the presence of metallic Cu peaks for both as-deposited and imprinted samples. However, the latter peak was weak for the imprinted

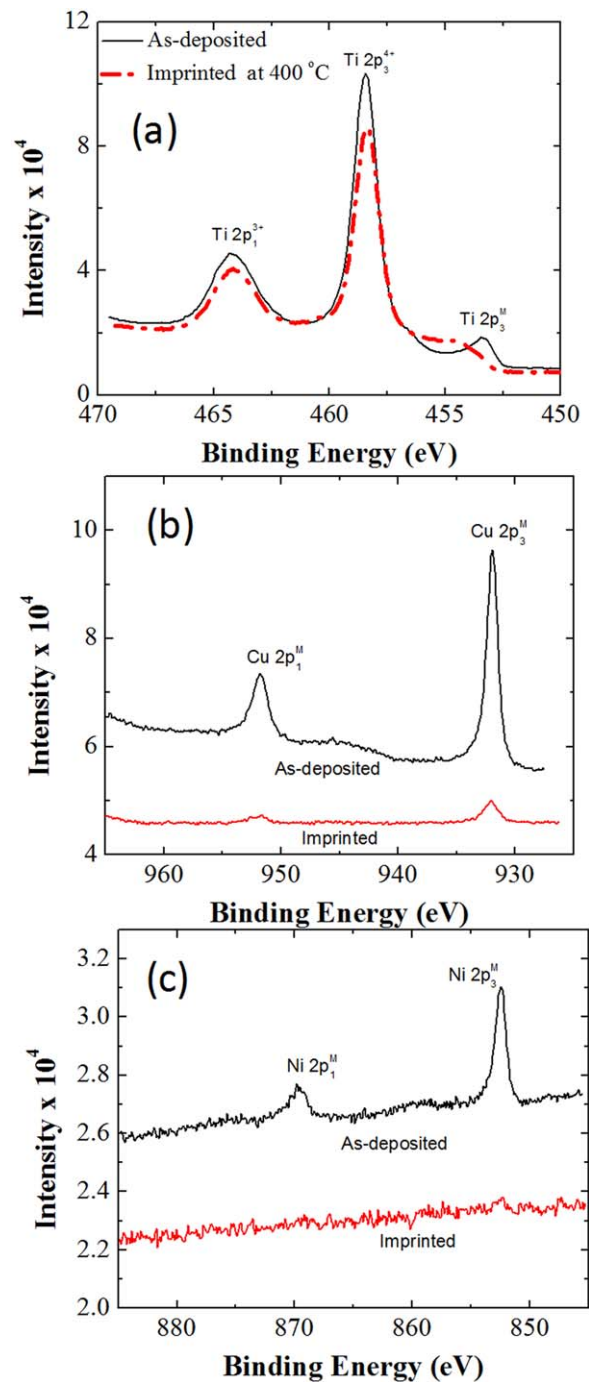


FIGURE 4. Detailed XPS of (a) Ti, (b) Cu, and (c) Ni in TiCuNi thin films in as deposited and imprinted state (imprinting temperature was 400°C). It shows that the upper surface of TiCuNi is mainly made up of titanium oxide (analysis depth of XPS is ~10 nm). [Color figure can be viewed in the online issue, which is available at wileyonlinelibrary.com.]

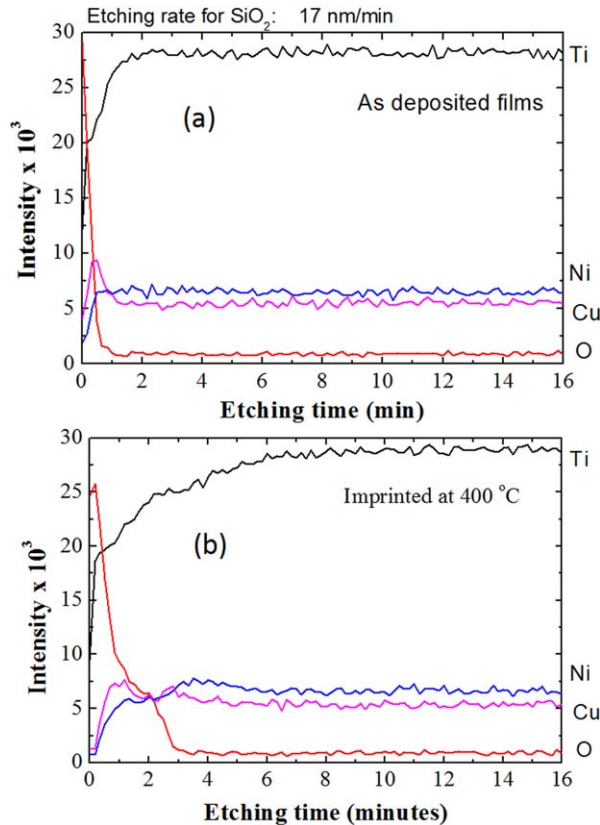


FIGURE 5. AES relative compositional depth profiles for (a) as deposited, and (b) imprinted (at 400°C) TiCuNi thin films. [Color figure can be viewed in the online issue, which is available at wileyonlinelibrary.com.]

samples. Taken together, the surface of as-deposited films was mainly consisted of thin passivation layer of Ti oxide.

Auger electron spectroscopy (JAMP-7100E, JEOL, Japan) in combination with Ar-ion beam sputtering were used to analyze the presence of different elements on the surface and beneath of as-deposited and imprinted TiCuNi metallic glass thin films. Figure 5(a,b) show the compositional depth profiles of as-deposited and imprinted TiCuNi films. Variation of Ti, Cu, Ni, and oxygen contents with the Ar-ion etching time was also assessed. The top surface of as-deposited film contains mainly Ti and oxygen and some small traces of Cu and Ni. As the etching time was increased, the oxygen content was sharply decreased for the as-deposited thin film. After one minute of etching, the oxygen level in the film was dropped close to the background level. However, the relative amounts of all other elements were remained almost similar with regard to further etching [Figure 5(a)]. For the imprinted TiCuNi sample, the top surface was also composed of Ti and oxygen. It should be noticed that with the imprinting, the Cu content was suppressed to a noticeable level and the oxygen signal reached to the background level after the etching time of ~ 3 min. Under these etching conditions, the etching rate for SiO_2 was $\sim 17 \text{ nm min}^{-1}$. The etching rate generally depends on the elements and their phases and metals usually have a higher etching rate than the oxides.

Mechanical properties

Excessive wear of Ti-based alloys is an important characteristic of these materials. Wear resistance is different for different materials and depends on mechanical hardness and surface properties. For traditional materials both theory and experiments showed that the wear resistance increases with hardness,^{52,53} but some exceptional reports also exist.⁵² For metallic glasses, wear resistance is usually shown to increase with increase in hardness.⁵⁴ Figure 6(a) shows the loading and un-loading curves for the TiCuNi film of thickness $\sim 3.5 \mu\text{m}$ obtained from the nano-mechanical testing. Inset picture shows the typical shape of the indentation at a load of 5 mN. Well-defined pop-ins and pile-up of material outside the indent were noticeable in accordance with other metallic glasses.⁵⁵ The average mechanical hardness (H) and reduced Young's modulus (E_r) obtained from independent experiments were ~ 6.9 and 130 GPa, respectively.

Wear resistance on the TiCuNi thin films were performed by measuring the depth of a worn square pattern [inset of Figure 6(b)] of size $\sim 1 \times 1 \mu\text{m}^2$ at different loads. Scanning was done at each load with a Berkovich diamond

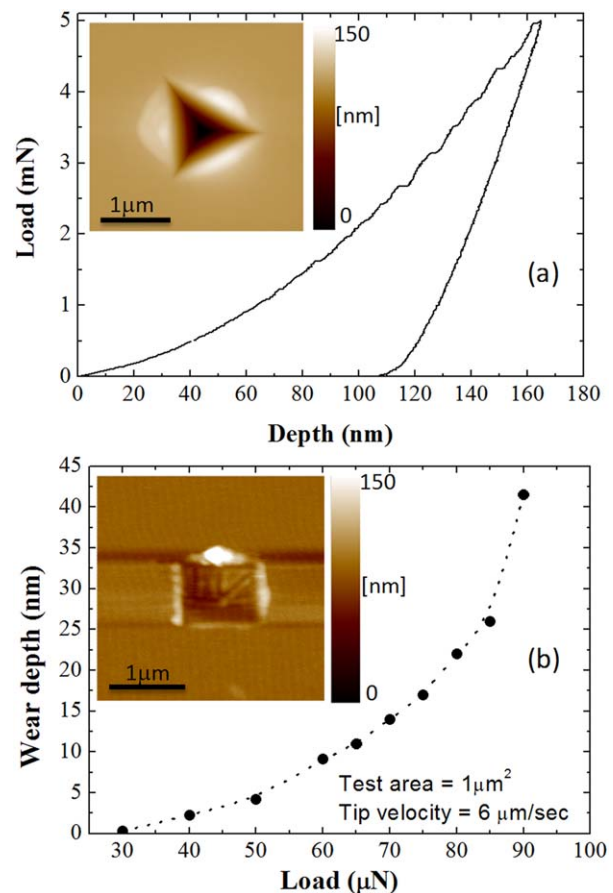


FIGURE 6. (a) Typical load-displacement curve on a TiCuNi thin film showing well defined pop-ins. Inset shows the scanning probe microscope (SPM) image of an indent. Pileup of material around the indent is typical for glassy materials. (b) Shows the dependence of wear depth on applied load. SPM image in inset is the typical shape of the worn out pattern. [Color figure can be viewed in the online issue, which is available at wileyonlinelibrary.com.]

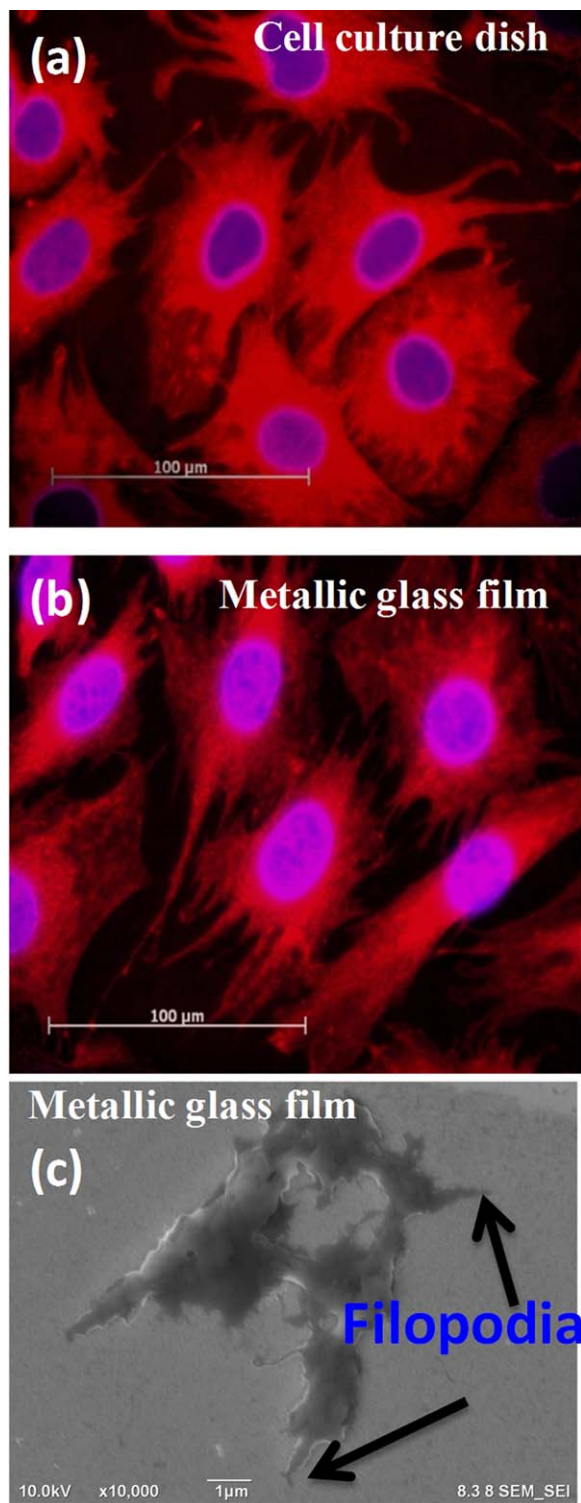


FIGURE 7. Fluorescence microscope images of muscle cells cultured on (a) the conventional cell culture dish and (b) metallic glass thin film. Cell nuclei and F-actin were stained as blue and red, respectively. (c) SEM image of the cells cultured on a metallic glass thin film. [Color figure can be viewed in the online issue, which is available at wileyonlinelibrary.com.]

nano-indenter. A nonuniform wear of the film was noticed from the image as shown in the inset of Figure 6(b) and the line profile (not shown here). This wear behavior is similar

to the amorphous carbon films. However, the wear depths in the case of TiCuNi thin films were significantly lower than the amorphous carbon. A wear depth of ~ 2.5 nm was noticed at the load of ~ 17 μN in the case of amorphous carbon, but the glassy TiCuNi films did not show any signs of wear at this load. We did not observe wear-up of the film up to the load of ~ 30 μN . Above this amount of load, the wear depth was increased slowly till the thickness of ~ 15 nm, and after that it was increased rapidly with the adding loads. A nonlinear dependence of the wear depth with the applied load was recorded as demonstrated in Figure 6(b). A significantly high wear resistance up to the thickness of ~ 15 nm was likely due to the presence of titanium oxide as confirmed with the XPS analysis. It is well known that the surface oxidation of Ti-based alloys is effective in increasing the hardness and thereby the wear resistance.⁵⁶

It is worth mentioning that we have deposited metallic glass thin films of different alloy systems on a variety of substrates such as conventional silica glass, silicon, metals and polymers. On the basis of the simple scratch and adhesive tape tests in our laboratory, we can say that metallic glass thin films have very good adhesion on metals,

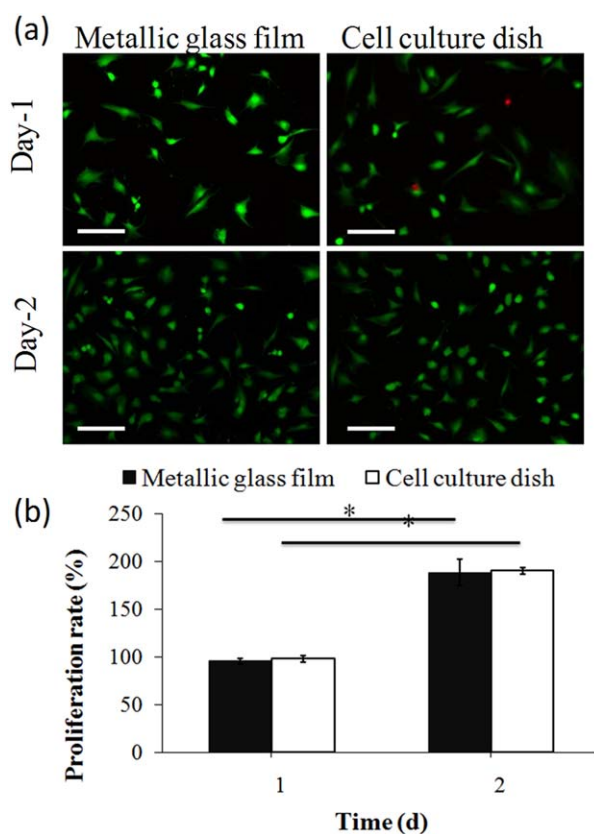


FIGURE 8. (a) Fluorescence microscopic images of muscle cells on the metallic glass thin film and the conventional cell culture dish after 1 and 2 days of cell culture. Scale bar corresponds to 100 μm . Live and dead cells were stained as green and red, respectively. (b) Proliferation rate of muscle cells on metallic glass thin film and cell culture dish. Cells almost duplicated their populations after 2 days of culture ($*p < 0.05$). [Color figure can be viewed in the online issue, which is available at wileyonlinelibrary.com.]

semiconductors and oxide substrates. Reasonably good adhesion was also obtained on polymer substrates.^{57,58}

Biocompatibility of metallic glass thin films

To investigate the biocompatibility of metallic glass thin films, the muscle cells grown on these films were stained with DAPI and phalloidin after 1 day of culture to reveal cell nuclei and F-actin, respectively. For control experiments, the same procedure was done for the cells grown on the conventional cell culture dishes. The results are demonstrated in Figure 7. As can be seen, there is no cytotoxicity effect of metallic glass thin films on the C2C12 myoblasts. The muscle cells on both substrates, that is, metallic glass thin films and cell culture dishes started to elongate and communicate with other cells. SEM pictures of cells on the metallic glass thin films also confirmed the biocompatibility of these substrates [Figure 7(c)]. We also observed that the cells on the metallic glass films were able to proliferate well. The latter phenomenon was quantified as to count the number of live cells on both metallic glass thin films and cell culture dishes after 1 and 2 days of culture. Here, the proliferation rate was defined as the ratio of number of live cells to the total number of cells at day 1 of culture. As can be seen from Figure 8, almost all cells on both metallic glass substrates and cell culture dishes remained alive after 1 day of culture and they almost duplicated their populations after 2 days of culture. Taken together, the metallic glass substrates showed good biocompatibility as exposed to muscle cells *in vitro* indicating the great promise of these materials for biomedical applications.

CONCLUSIONS

The films of TiCuNi were deposited by the sputtering technique on the Si substrate. Films were structurally amorphous and had high mechanical and wear resistant properties. *In vitro* biocompatibility analysis confirmed that these films are nontoxic to the mammalian cells and are suitable for the cell growth and tissue formation. Polymer-like imprintability of TiCuNi metallic glass thin films confirmed that they could satisfy required precision and repeatability to shape intricate geometries used in biomedical applications. Also, they can coat any non-biocompatible material or device for biomedical applications.

ACKNOWLEDGMENTS

The authors thank Prof. M. W. Chen and Mr. K. Madhav Reddy at WPI-AIMR, Tohoku University for his help during SEM imaging of muscle cells [Figure 7(c)].

REFERENCES

- Wang M. Developing bioactive composite materials for tissue replacement. *Biomaterials* 2003;24:2133.
- Ratner BD, Hoffman AS, Schoen FJ, Lemmon JE. *Biomaterials Science: An Introduction to Materials in Medicine*, 2nd ed. Orlando, FL: Academic Press; 2004.
- Navarro M, Michiardi A, Castano O, Planell JA. Biomaterials in orthopaedics. *J R Soc Interface* 2008;5:1137.
- Wise DL, Trantolo DJ, Altobelli DE, Yaszemsk MJ, Grasser JD. *Human Biomaterials Applications*. Totowa, NJ: Humana Press; 1996.
- Schroers J, Kumar G, Hodges TM, Chan S, Kyriakides TR. Bulk metallic glasses for biomedical applications. *JOM* 2009;61:21.
- Sharma P, Kaushik N, Kimura H, Saotome Y, Inoue A. Nano-fabrication with metallic glass—An exotic material for nano-electromechanical systems. *Nanotechnology* 2007;18:035302.
- Saotome Y, Hatori T, Zhang T, Inoue A. Super plastic micro/nano-formability of La₆₀Al₂₀Ni₁₀Co₅Cu₅ amorphous alloy in supercooled liquid state. *Mater Sci Eng A* 2001;304:716–720.
- Kumar G, Tang HX, Schroers J. Nanomoulding with amorphous metals. *Nature* 2009;457:868–872.
- Truckenmuller R, Giselsbrecht S, Rivron N, Gottwald E, Saile V, Berg A, Wessling M, Blitterswijk C. Thermoforming of film-based biomedical microdevices. *Adv Mater* 2011;23:1311–1329.
- Zhang T, Inoue A, Masumoto T. The effect of atomic size on the stability of super cooled liquid for amorphous (Ti, Zr, Hf) 65Ni₂₅Al₁₀ and (Ti, Zr, Hf) 65Cu₂₅Al₁₀ alloys. *Mater Lett* 1993;15:379–382.
- Tanner LE, Ray R. Physical properties of Ti₅₀Be₄₀Zr₁₀ glass. *Scripta Mater* 1977;11:783–789.
- Inoue A, Zhang W, Zhang T, Kurosaka K. Cu-based bulk glassy alloys with high tensile strength of over 2000 MPa. *J Non-Cryst Solids* 2002;304:200–209.
- Inoue A, Zhang T, Masumoto T. Zr-Al-Ni amorphous-alloys with high glass-transition temperature and significant supercooled liquid region. *Mater Trans JIM* 1990;31:177–183.
- Jin K, Löffler JF. Bulk metallic glass formation in Zr-Cu-Fe-Al alloys. *Appl Phys Lett* 2005;86:241909.
- Peker A, Johnson WL. A highly processable metallic-glass Zr_{41.2}Ti_{13.8}Cu_{12.5}Ni_{10.0}Be_{22.5}. *Appl Phys Lett* 1993;63:2342–2344.
- Ponnambalam V, Poon SJ, Shiflet GJ. Fe-Mn-Cr-Mo-(Y,Ln)-C-B (Ln = lanthanides) bulk metallic glasses as formable amorphous steel alloys. *J Mater Res* 2004;19:3046–3052.
- Lu ZP, et al. Structural amorphous steels. *Phys Rev Lett* 2004;92:245503.
- Zhang QS, Zhang W, Inoue A. New Cu-Zr based bulk metallic glasses with large diameters of up to 1.5 cm. *Scripta Mater* 2006;55:711–713.
- Xu DH, et al. Formation and properties of new Ni-based amorphous alloys with critical casting thickness up to 5 mm. *Acta Mater* 2004;52:3493–3497.
- Lin XH, Johnson WL. Formation of Ti-Zr-Cu-Ni bulk metallic glasses. *J Appl Phys* 1995;78:6514–6519.
- Inoue A, et al. Mg-Cu-Y Amorphous-alloys with high mechanical strengths produced by a metallic mold casting method. *Mater Trans JIM* 1991;32:609–616.
- Nishiyama N, Inoue A. Supercooling investigation and critical cooling rate for glass formation in P-Cu-Ni-P alloy. *Acta Mater* 1999;47:1487–1495.
- Schroers J, et al. Gold based bulk metallic glass. *Appl Phys Lett* 2005;87:061912.
- Schroers J, Johnson WL. Highly processable bulk metallic glass-forming alloys in the Pt-Co-Ni-Cu-P system. *Appl Phys Lett* 2004;84:3666–3668.
- Gu X, Zheng Y, Zhong S, Xi T, Wang J, Wang W. Corrosion of and cellular response to Mg-Zn-Ca bulk metallic glasses. *Biomaterials* 2010;31:1093–1103.
- Buzzi S, Jin K, Uggowitzer PJ, Tosatti S, Gerber I, Löffler JF. Cytotoxicity of Zr-based bulk metallic glasses. *Intermetallics* 2006;14:729–734.
- Lui L, Qui CL, Huang CY, Yu Y, Huang H, Zhang SM. Biocompatibility of Ni-free Zr-based bulk metallic glasses. *Intermetallics* 2009;17:234–240.
- Kim YC, Kim WT, Kim DH. A development of Ti-based bulk metallic glass. *Mater Sci Eng A* 2004;375–377:127–135.
- Xie KF, Yao KF, Huang TY. A Ti-based bulk glassy alloy with high strength and good glass forming ability. *Intermetallics* 2010;18:1837–1841.
- Zhu SL, Wang XM, Inoue A. Glass forming ability and mechanical properties of Ti-based bulk glassy alloys with large diameters up to 1 cm. *Intermetallics* 2008;16:1031–1035.
- Ahadian S, Hosseini V, Ostrovidov S, Camci-Unal G, Chen S, Kaji H, Ramalingam M, Khademhosseini A. Engineered contractile skeletal muscle tissue on a microgrooved methacrylated gelatin substrate. *Tissue Eng A* 2012;18:2453.

32. Ramón-Azcón J, Ahadian S, Obregón R, Camci-Unal G, Ostrovidov S, Hosseini V, Kaji H, Ino K, Shiku H, Khademhosseini A, Matsue T. Gelatin methacrylate as a promising hydrogel for 3D microscale organization and proliferation of dielectrophoretically patterned cells. *Lab Chip* 2012;12:2959.
33. Ahadian S, Ramón-Azcón J, Ostrovidov S, Camci-Unal G, Hosseini V, Kaji H, Ino K, Shiku H, Khademhosseini A, Matsue T. Interdigitated array of Pt electrodes for electrical stimulation and engineering of aligned muscle tissue. *Lab Chip* 2012;12:3491.
34. Ahadian S, Ramón-Azcón J, Ostrovidov S, Camci-Unal G, Kaji H, Ino K, Shiku H, Khademhosseini A, Matsue T. A contactless electrical stimulator: Application to fabricate functional skeletal muscle tissue. *Biomed Microdev.* 2013;15:109–115.
35. Azcon JR, Ahadian S, Estili M, Liang X, Ostrovidov S, Kaji H, Shiku H, Ramalingam M, Nakajima K, Sakka Y, Khademhosseini A, Matsue T. Dielectrophoretically aligned carbon nanotubes to control electrical and mechanical properties of hydrogels to fabricate contractile muscle myofibers. *Adv Mater* 2013;15:4028–4034.
36. Ahadian S, Ostrovidov S, Hosseini V, Kaji H, Ramalingam M, Bae H, Khademhosseini A. Electrical stimulation as a biomimicry tool for regulating muscle cell behavior. *Organogenesis* 2013;2:87–92.
37. Murtuza B, Nichol JW, Khademhosseini A. Micro- and nanoscale control of the cardiac stem cell niche for tissue fabrication. *Tissue Eng B Rev* 2009;15:443.
38. Khademhosseini A, Eng G, Yeh J, Kucharczyk PA, Langer R, Vunjak-Novakovic G, Radisic M. Microfluidic patterning for fabrication of contractile cardiac organoids. *Biomed Microdev* 2007;9:149.
39. Gerber H, Perren SM. Evaluation of tissue compatibility of in vitro cultures of embryonic bone. In: Winter GD, Leray JL, de Groot K, editors. *New York: Wiley; 1980.* pp 307–314.
40. Peltonen L. Nickel sensitivity in general population. *Contact Dermatitis* 1979;5:23–27.
41. Castlemen LS, Motzkin SM, Alicandri FP, Bonawit VL. Biocompatibility of nitinol alloy as an implant material. *J Biomed Mater Res* 1976;10:695–731.
42. Puffers JL, Kaulesar Sukul DM, de Zeeuw GR, Bijma A, Besselink PA. Comparative cell culture effects of shape memory metal (Nitinol), nickel and titanium: A biocompatibility estimation. *Eur Surg Res* 1992;24:378–382.
43. Cutright DE, Bhaskar SN, Perez B, Johnson RM, Cowan GS. Tissue reaction to nitinol wire alloy. *Oral Surg Oral Med Oral Pathol* 1973;35:578–584.
44. Shin SR, Jung SM, Zalabany M, Kim K, Zorlutuna P, Kim SB, Nikkhah M, Khabiry M, Azize M, Kong J, Wan K-T, Palacios T, Dokmeci MR, Bae H, Tang X, Khademhosseini A. Carbon-nanotube-embedded hydrogel sheets for engineering cardiac constructs and bioactuators. *ACS Nano* 2013;7:2369.
45. Shin SR, Bae H, Cha JM, Mun JY, Chen Y-C, Tekin H, Shin H, Farshchi S, Dokmeci MR, Tang S, Khademhosseini A. Carbon-nanotube-embedded hydrogel sheets for engineering cardiac constructs and bioactuators. *ACS Nano* 2012;6:362.
46. Sharma P, Zhang W, Amiya K, Kimura H, Inoue A. Nanoscale patterning of ZrAlCuNi metallic glass thin films deposited by magnetron sputtering. *J Nanosci Nanotechnol* 2005;5:416–420.
47. Shen XJ, Pan LW, Lin L. Microplastic embossing process: Experimental and theoretical characterization. *Sens Actuators A* 2002;97/98:428.
48. Rowland HD, Sun AC, Schunk PR, King WP. Impact of polymer film thickness and cavity size on the polymer flow during embossing: Toward process design rules for nanoimprint lithography. *J Micromech Mecroeng* 2005;15:2414.
49. Saotome Y, Imai K, Sawanobori N. Microformability of optical glasses for precision molding. *J Mater Process Technol* 2003;140:379–384.
50. Huang X, Ramirez AG. Structural relaxation and crystallization of NiTi thin film metallic glasses. *Appl Phys Lett* 2009;95:121911.
51. Chui CL, Chung CY, Chu PK. Surface oxidation of NiTi shape memory alloy in a boiling aqueous solution containing hydrogen peroxide. *Mater Sci Eng A* 2006;417:104–109.
52. Qian L, Xiao X, Sun Q, Yu T. Anomalous relationship between hardness and wear properties of superelastic nickel-titanium alloy. *Appl Phys Letts* 2004;84:1076.
53. Dhokey NB, Rane KK. Wear behavior and its correlation with mechanical properties of TiB₂ reinforced aluminum-based composites. *Adv Tribol* 2011;2011:1–8.
54. Togashi N, Ishida M, Nishiyama N, Inoue A. Wear resistance of metallic glass bearings. *Rev Adv Mater Sci* 2008;18:93–97.
55. Sharma P, Yubuta K, Kimura H, Inoue A. Brittle metallic glass deforms plastically at room temperature in glassy multilayers. *Phys Rev B* 2009;80:024106.
56. “Wear testing at nanoscale” Available at: <http://www.hysitron.com/applications/material-properties/scratch-and-wear-resistance>.
57. Soinila E, Sharma P, Heino M, Pischow K, Inoue A, Hanninen H. Bulk metallic glass coating on polymer substrate. *J Phys Conf Ser* 2009;144:012051.
58. Sharma P, Inoue A. *Metallic Glasses in Handbook of Silicon based MEMS Materials and Technologies. A Volume on Micro and Nanotechnologies.* William Andrew Applied Science Publisher (India: Elsevier); 2010. pp 447–472; Chapter 27.